Drug Design, Development and Therapy

Dovepress
open access to scientific and medical research

Open Access Full Text Article

ORIGINAL RESEARCH

Mechanism Investigation and Clinical Retrospective Evaluation of Qingyi Granules: Pancreas Cleaner About Ameliorating Severe Acute Pancreatitis with Acute Respiratory Distress Syndrome

Peng Ge[1–3,*], Yalan Luo[3,*], Jinquan Zhang[1–3,*], Jie Liu[1–3], Caiming Xu[1,4], Haoya Guo[1–3], Aixia Gong[3], Guixin Zhang[1–3], Hailong Chen[1–3]

[1]Department of General Surgery, The First Affiliated Hospital of Dalian Medical University, Dalian, Liaoning, People's Republic of China; [2]Institute (College) of Integrative Medicine, Dalian Medical University, Dalian, Liaoning, People's Republic of China; [3]Laboratory of Integrative Medicine, The First Affiliated Hospital of Dalian Medical University, Dalian, Liaoning, People's Republic of China; [4]Department of Molecular Diagnostics and Experimental Therapeutics, Beckman Research Institute of City of Hope, Biomedical Research Center, Comprehensive Cancer Center, Duarte, CA, USA

*These authors contributed equally to this work

Correspondence: Guixin Zhang; Hailong Chen, Email zgx0109@126.com; chenhailong@dmu.edu.cn

Background: Despite its extensive utilization in Chinese hospitals for treating acute pancreatitis (AP) and related acute respiratory distress syndrome (ARDS), the active components and mechanisms underlying the action of Qingyi Granule (QYKL) remain elusive.
Methods: This study consists of four parts. First, we used Mendelian randomization (MR) to investigate the causal relationship between AP, cytokine, and ARDS. Next, 321 patients were collected to evaluate the efficacy of QYKL combined with dexamethasone (DEX) in treating AP. In addition, we used UHPLC-QE-MS to determine the chemical constituents of QYKL extract and rat serum after the oral administration of QYKL. The weighted gene coexpression network analysis (WGCNA) method was used to find the main targets of AP-related ARDS using the GSE151572 dataset. At last, a AP model was established by retrograde injection of 5% sodium taurocholate.
Results: MR showed that AP may have a causal relationship with ARDS by mediating cytokine storms. Retrospective study results showed early administration of QYKL was associated with a lower incidence of ARDS, mortality, admissions to the intensive care unit, and length of stay in AP patients compared to the Control group. Furthermore, we identified 23 QYKL prototype components absorbed into rat serum. WGCNA and differential expression analysis identified 1558 APALI-related genes. The prototype components exhibited strong binding activity with critical targets. QYKL has a significant protective effect on pancreatic and lung injury in AP rats, and the effect is more effective after combined treatment with DEX, which may be related to the regulation of the IL-6/STAT3 signaling pathway.
Conclusion: By integrating MR, retrospective analysis, and systematic pharmacological methodologies, this study systematically elucidated the therapeutic efficacy of QYKL in treating AP-related ARDS, establishing a solid foundation for its medicinal use.
Keywords: acute pancreatitis, qingyi granule, dexamethasone, acute lung injury, clinical efficacy, Mendelian randomization, rat

Introduction

With population growth changes in the environment (including changes in dietary patterns, increasing obesity rates, smoking, and other factors), the current global incidence of AP is increasing year by year, reaching 34 patients per 100,000 population per year (95% CI: 23–49), and the mortality rate got 1.16 per 100,000 people per year (95% CI: 0. 85–1. 58).[1] A survey found that the total hospitalization expenditure for patients with AP in the United States in 2003 was as high as US$2.2 billion (95% confidence interval of US$2 billion to US$2.3 billion), with an average of US $1,670 per hospital day (95% confidence interval of US$1620-1720).[2] The average cost per hospitalization is nearly

Received: 8 January 2024
Accepted: 9 May 2024
Published: 7 June 2024

Graphical Abstract

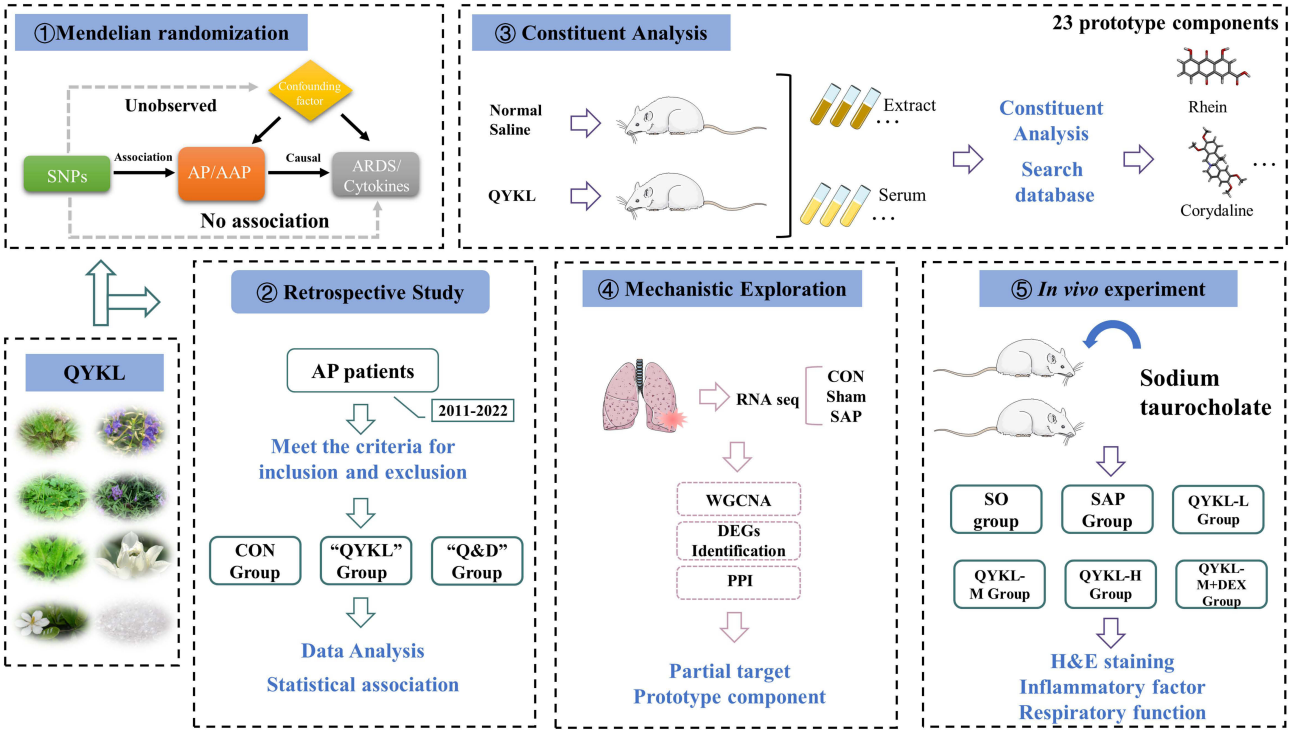

10,000 US dollars, which has become a significant burden on national medical expenses.[2] Reducing hospital expenses is very important. Approximately 80% of clinical AP patients belong to mild acute pancreatitis (MAP), which could be cured by conservative treatment without any complications remaining; the other 20% of AP patients are afflicted by moderate or severe acute pancreatitis, which usually contributes to complications, including systemic inflammatory response syndrome (SIRS) and distal organ damage, such as acute lung injury (ALI) or acute respiratory distress syndrome (ARDS).[3] Therefore, the ability to limit AP to the early stage of ARDS is of great significance to patient prognosis and the social economy.

Qingyi decoction (QYD) is an optional traditional Chinese medicine prescription for the treatment of AP, which is modified by the combination of Dachengqi decoction and Dachaihu decoction, containing Scutellaria baicalensis, Fructus Gardeniae, Rhizoma corydalis, Radix bupleuri, Rheum officinale, Radix paeoniae alba, Natrii Sulfas, and Costustoot.[4] From the perspective of modern medicine, QYD plays an essential role in inhibiting inflammation, relaxing the Oddi sphincter, relieving spasms, inhibiting pancreatic enzyme secretion, promoting gastrointestinal motility, maintaining the intestinal barrier, and protecting the functions of the other organs.[4–7] Our hospital has developed the "Qingyi granule/ Qingyi Keli (QYKL)" preparation based on QYD, and this preparation has the characteristics of standardized production, convenient consumption, and stable composition. It has achieved effects in clinical practice to some degree. However, the effectiveness of QYKL has been noticed, and its material basis needs to be further studied. Prior research has analyzed the chemical components present in QYD using liquid chromatography-mass spectrometry.[8] Additionally, the molecular mechanism of QYD's efficacy in treating AP and related ALI has been elucidated through network pharmacology.[9] Pharmaceutical chemists believe that for drugs to effectively exert their therapeutic effects in the human body, they must first enter the bloodstream. QYKL is primarily administered orally and exerts its pharmacological effects upon entering the bloodstream through the enterohepatic circulation. Consequently, it is crucial to identify the prototype constituents of QYKL absorbed into the serum to understand its mechanism of action.

Mendelian randomization (MR), which eliminates the possibility of reverse causation and confounding factors, has been more popular in recent years to establish the relationship between two phenotypes.[10] To establish the link between AP, cytokine storm, and ARDS, we initially used the MR method. Furthermore, we explore the effects of QYKL combined with dexamethasone (DEX) on inflammatory response indicators, biochemical indicators, and clinical efficacy and determine the social and economic benefits in patients with AP. The mechanism of QYKL is unknown, and its composition is complex. The prototype constituents of QYKL absorbed into the serum were identified by Ultra-high-performance liquid chromatography/Q Exactive HFX mass spectrometer (UHPLC-QE-MS), and the mechanism of QYKL intervention on APALI was analyzed by network pharmacology. In vivo experiments were conducted to validate the findings further.

Materials and Methods

MR

In this study's MR analysis, genetic variants such as single nucleotide polymorphisms (SNPs) were used as instrumental variables (IVs), AP was used as the exposure, and ALI/ARDS and cytokines were the outcomes. MR analysis must satisfy three fundamental assumptions: 1) The "correlation" hypothesis: IVs and AP are highly correlated; 2) The "exclusivity" hypothesis: IVs are not directly related to outcome and can only be associated with outcome via exposure; and 3) The "independence" hypothesis: IVs is not associated with confounding factors associated with the exposure and outcome. The GWAS data for AP, alcoholic acute pancreatitis (AAP), ARDS, pleural effusion, and pulmonary oedema were obtained from the IEU Open GWAS project. From 8293 participants in three independent cohort studies, we obtained GWAS summary statistics for 41 cytokine concentrations in circulation.[11] Because the data above are from public sources, we do not need extra ethical permission for further study.

We lower the "correlation" hypothesis threshold to less than 5E-06 to include more candidate SNPs. We estimated the Linkage disequilibrium (LD) between SNPs using a reference cohort from 1000 Genomes EUR. We retained SNPs with $r^2 = 0.01$ and clumping distance = 1000. Candidate SNPs were matched with GWAS summary statistics for outcomes based on chromosome and location. SNPs that were closely related to the results were excluded($P < 5E-08$). In addition, the F statistic was used to evaluate the IVs' efficacy. IVs with a F value of less than ten are eliminated. The formula is $F=\beta^2/se^2$, where β is the effect value of the allele and se is the standard error.

In the MR analysis, we used inverse variance weighted (IVW) to assess the causal relationship between exposure and outcome. $P < 0.05$ indicated the significance of the causal relationship. MR-egger regression, simple mode, weighted mode and weighted median (WME) methods are additional methods, and the results are considered reliable when they are consistent with the effect direction obtained by IVW. We also conducted sensitivity analyses supported by multiple methodologies to determine whether IVs exhibit heterogeneity and pleiotropy. The heterogeneity of IVs was evaluated using Cochran's Q test, with $P < 0.05$ indicating heterogeneity. Horizontal pleiotropy was assessed using the intercept of IVs in MR-egger regression, with $P < 0.05$ indicating the presence of horizontal pleiotropy. The MR pleiotropy residual sum and outlier (MR-PRESSO) test examines and calibrates horizontal pleiotropy outliers. The relative risk was estimated using odds ratio (OR) and 95% Confidence interval (CI). For MR analysis in R version 4.1.2, the "TwosampleMR" and "MR-PRESSO" packages are utilized.

Retrospective Study

All data in this study were derived from the First Affiliated Hospital of Dalian Medical University, including the Abdominal Emergency Surgery Department, Emergency ICU, and Intensive Care Department. A total of 331 AP patients admitted to our hospital from May 2011 to May 2022 were included. After excluding 10 patients, the remaining 321 patients were included in the study. There were 222 men (69.16%) in the study. The patients were aged 19–98 years (average age 54.44 ± 17.51 years). When admitted to the hospital, 226 patients had nausea and vomiting symptoms (70.40%), and 27 patients had a previous surgical history (8.41%). Ethical approval was obtained by the First Affiliated Hospital of Dalian Medical University (Ethics No. PJ-KS-KY-2021-283). This study was registered with the Chinese Clinical Trial Registry on July 11, 2022, under the registration number ChiCTR2200061929. In addition, the necessity

for patients' informed permission was removed due to the investigation's retrospective character. Diagnostic criteria, inclusion and exclusion criteria of cases, grouping, and observation indicators are shown in Supplementary Method S1.

Studies on the Ingredients Absorbed into the Serum of QYKL

Liaoning Changsheng Biotechnology Co., LTD provided twelve SPF-grade Male Sprague-Dawley (SD) rats aged 6–8 weeks. The rats were reared at Dalian Medical University's SPF Laboratory Animal Centre. Temperature 22 ± 2 °C, 60 ± 10% humidity, 12 h light and dark cycle, accessible nutrition, and drinking water were the feeding conditions. The experiment was carried out with the agreement of Dalian Medical University's Experimental Animal Ethics Committee, and it satisfied the Guidelines for the Care and Use of Laboratory Animals developed by the National Institutes of Health, USA. The rats were randomly divided into the blank group (n = 6) and the QYKL group (n = 6). The QYKL group was administrated with QYKL, and the blank group was given normal saline of the same volume. The QYKL or saline was given intragastrically for a week (once in the morning and once in the evening, 10 mL/kg). At 1.5–2 h after the last administration, isoflurane-inhaled anesthetized rats were disinfected. The abdominal aorta blood was collected, placed at room temperature for 2 h, and then centrifuged for 10 min at 4 °C and 3500 rpm. The resulting serum was reserved, subpackaged, and stored at −80 °C. Details of the materials, instruments, and methods required for mass spectrometry are provided in Supplementary Method S2.

Network Pharmacology

Screening of APALI-Related Genes

Sequencing data (GSE151572) of SAP rat lung tissue were obtained from the GEO database. The sequencing platform was GPL24688. The WGCNA analysis included: 1) Genes with low average expression were removed, and the top 5000 genes with average expression were selected; 2) Cluster samples and eliminate outlier samples; 3) Suitable soft thresholds were screened to construct scale-free networks, and the fitting index was set as R^2 greater than or equal to 0.85, the minimum number of module genes was 100, and the threshold for merging similar modules was 0.25; 4) The correlation between modules and the SAP group was calculated.

The module with the highest correlation with disease and a P value equal to or lesser than 0.05 was the disease-specific module; 5) gene significance (GS) and module membership (MM) were calculated to screen genes in the module, and the range was set as MM greater than or equal to 0.8 and the absolute value of GS greater than or equal to 0.2. The differentially expressed genes (DEGs) between SAP and control rat lung tissues were analyzed and identified. The threshold was set as a P value less than 0.05, and the absolute value of log2 (fold change) was more significant than 0.58.

Target Prediction of Prototype Constituents

First, the prototype constituents' pharmacokinetic data were obtained from the SwissADME database,[12] and the components that did not satisfy the criteria were eliminated using the Lipinski rules. Subsequently, potential targets of prototype components are obtained from TCMSP,[13] HERB, and SwissTargetPrediction (STP)[14] databases. Similarly, the target names are standardized using the UniProt database. A Venn diagram was created to ascertain the intersection of prototype constituent targets and APALI targets.

PPI Network Construction

The shared targets were imported into the STRING database, the species was set as "Homo sapiens", and the interaction information between the various targets was downloaded—construction of a PPI network with the shared target using Cytoscape 3.8.2 software. Cytohubba plugin was used to analyze the topological parameter degree of each target to identify the core targets.

Functional Enrichment Analysis

The shared targets were imported into the DAVID database for enrichment analysis of Gene Ontology (GO) biological function and Kyoto Encyclopedia of Genes and Genomes (KEGG) signaling pathway. Terms with P values less than 0.05 are deemed to have biological significance.

Molecular Docking

The structure of all prototype components can be downloaded from the PubChem database. The RCSB PDB database is searched for the crystal structures of key targets. The Autodock vina was utilized for molecular docking of prototype components and key targets, and the binding energy was determined.

In vivo Study

Grouping and Treatment Procedures

Sixty rats were randomly allocated into different groups, including a sham operation (SO) group, a SAP group, a low, medium, and high dose QYKL group, and a medium dose QYKL combined with the Dex group. Each group consisted of 10 rats. As mentioned earlier, The SAP model was constructed by injecting 5% sodium taurocholate into the bile pancreatic duct in a retrograde manner.[15] The SO group received an equivalent dosage of saline. The QYKL treatment group received intragastric administration of QYKL at low, medium, and high doses of 5, 10, and 15 g crude drug/kg, respectively, at 2 and 12 h after modeling. The DEX treatment group received intravenous administration of DEX (10 mg/kg) at 2 and 12 h after modeling. 24 h after the modeling procedure, six rats were euthanized in each experimental group. Serum, pancreatic, and lung tissue samples were collected from each rat and stored at −80 °C.

Histopathological Examination of the Pancreas and Lungs

A portion of the pancreas and lung from each group were immersed in a 4% paraformaldehyde solution for overnight fixation. The tissues underwent embedding in paraffin, slicing, dewaxing, dehydration, and consecutive staining with hematoxylin-eosin (HE). Histopathological changes were observed using an optical microscope. Indicators of pancreatic and lung tissue damage were determined using established criteria from previous publications.[16]

Blood Gas Analysis and Lung Wet-Dry Weight Ratio (W/D) Measurement

The blood gas analyzer measured the partial pressure of oxygen (PaO_2) and carbon dioxide ($PaCO_2$). The left upper lung of each group of rats was excised, rinsed with normal saline, and dried using sterile gauze. After measuring and documenting the initial weight, transfer the sample to an oven set at 60 °C for 24 h. Measure the weight of the dry sample and record the measurement. The formula for the wet weight ratio to dry weight (W/D) is given by W/D = wet weight / dry weight.

Determination of Amylase Activity, IL-1β, and TNFα Levels

Following the extraction of blood from the abdominal aorta, the blood samples were subsequently allowed to reach equilibrium with the ambient room temperature for 1 h. The supernatant was obtained through centrifugation at 3000 rpm and 4°C for 10 min. Serum amylase activity and levels of IL-1β and TNF-α were measured per the supplier's instructions.

Real Time-PCR

The concentration and purity of RNA extracted from 100 mg of lung tissue were measured. The RNA was reverse-transcribed into cDNA, followed by fluorescent quantitative PCR amplification. Internally, the reference gene was *gapdh. il*-6 primer sequence was Primer Forward: TAGTCCTCCCTACCCCAATTTCC; Primer Reverse: TTGGTCCTTAGCCACTCCTTC. There were three repetitions of the experiment.

Western Blot

From 100 mg of rat lung tissue, total protein was extracted. The BCA method was used to measure the total protein concentration. Electrophoresis using SDS-PAGE was used to transfer the proteins to PVDF membranes. After 5% skim

milk blocking, TBST washing, incubation of STAT3, p-STAT3 primary antibody (1:000 dilution), TBST washing, and incubation of secondary antibody (1:5000 dilution), ECL luminant was added to PVDF membrane. A gel imaging system exposed a PVDF membrane for development. The Image J program is used to analyze and calculate strip gray values.

Statistical Analysis

For statistical analysis, the software SPSS 24.0 was used. The data were expressed as mean±SD, one-way ANOVA was utilized for multi-group comparison, and the LSD-*t* test was utilized for two-group comparisons. It was statistically significant if $P < 0.05$.

Results

MR

ALI/ARDS and pleural effusion are common complications of AP. Based on the Berlin definition,[17] ALI/ARDS is diagnosed as follows: 1) acute onset: within 7 days of the onset of clinical impairment; 2) chest imaging: an infiltrative shadow that cannot be interpreted as a pulmonary nodule/pulmonary atelectasis; 3) respiratory failure that cannot be explained by heart failure or excessive fluid load; 4) oxygenation index (PaO_2/FiO_2) ≤300 mmHg at PEEP ≥5 cmH_2O. Consequently, ARDS, pleural effusion, and pulmonary edema were considered outcomes. All SNPs used to execute the MR analysis are described in Supplementary Table S1. All SNPs have F statistics greater than 10 (ranging from 20.86 to 91.64), indicating that weak IVs is less likely to cause bias.

There was no causal relationship between AP/AAP and ARDS, pleural effusion, and pulmonary edema and no evidence of heterogeneity or pleiotropic bias influencing the results according to Cochran's Q test, MR-egger regression analysis, and MR-PRESSO global test (Supplementary Table S2). The IVW analysis demonstrated a causal relationship between AP/AAP and elevated cytokine levels (Figure 1). MR-egger regression analysis and the WME method also validate the findings above (Figure 2). According to Cochran's Q test, MR-egger regression analysis, and MR-PRESSO global test (Supplementary Table S3), there was no evidence that heterogeneity or pleiotropic bias affected the study results.

Retrospective Study

A total of 331 patients with AP who met the research criteria were included in this study, of which 10 patients were dropped/excluded. The CON group included 133 patients, the QYKL group included 145 patients, and the Q&D group included 43 patients. General clinical features, comparison of baseline features between groups, and comparison of efficacy between groups based on GPSW are presented in Supplementary Tables S4–S7 and Supplementary Figure S1.

Exposure	Outcome	Method	P_value	OR (95% CI)
AP	Platelet−derived growth factor BB levels	IVW	0.037	1.087 (1.005 to 1.176)
	Interleukin−12p70 levels		0.039	1.086 (1.004 to 1.175)
	Interleukin−10 levels		0.013	1.108 (1.022 to 1.201)
	Interleukin−1−beta levels		0.039	1.128 (1.006 to 1.265)
	Interleukin−5 levels		0.010	1.182 (1.041 to 1.342)
	Interleukin−4 levels		0.001	1.154 (1.062 to 1.253)
	Fibroblast growth factor basic levels		0.047	1.088 (1.001 to 1.183)
AAP	Stem cell growth factor beta levels		0.041	1.093 (1.004 to 1.191)
	Monokine induced by gamma interferon levels		0.020	1.107 (1.016 to 1.206)
	Interleukin−12p70 levels		0.010	1.081 (1.019 to 1.146)
	Interleukin−10 levels		0.022	1.070 (1.010 to 1.133)
	Interleukin−8 levels		0.022	1.117 (1.016 to 1.228)
	Interleukin−1−beta levels		0.037	1.074 (1.004 to 1.149)

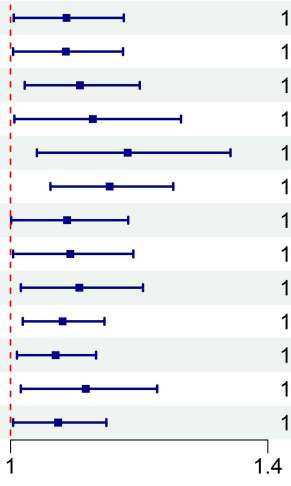

Figure 1 Forest plot of causality of AP/AAP on cytokine derived from Mendelian randomization analysis.
Abbreviations: AP, acute pancreatitis; AAP, alcoholic acute pancreatitis; IVW, inverse variance weighted; OR, odds ratio; CI, confidence interval.

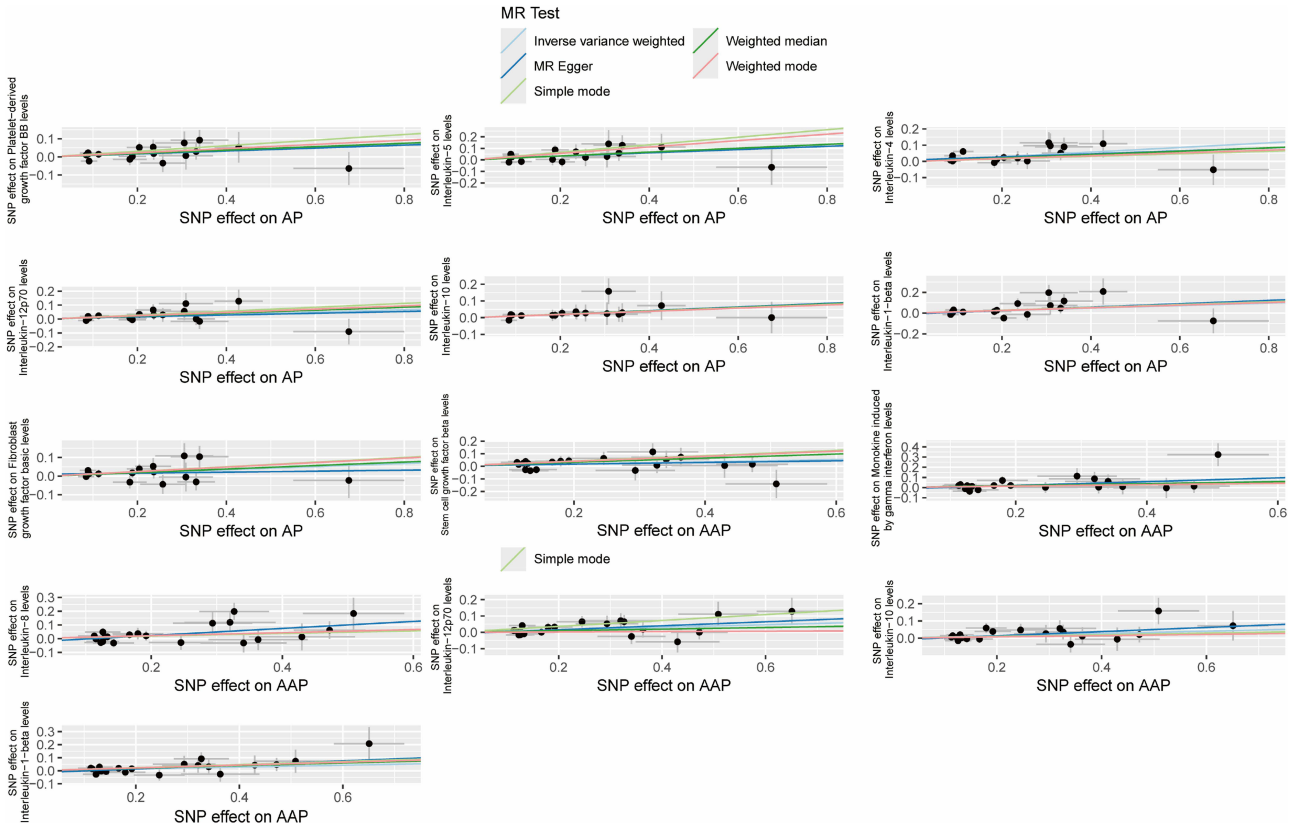

Figure 2 Scatter plot of Mendelian randomization association between AP/AAP and cytokines.
Abbreviations: AP, acute pancreatitis; AAP, alcoholic acute pancreatitis; SNP, single nucleotide polymorphism.

A GPSW-based logistic regression model was used to evaluate the therapeutic effect of the QYKL group and the Q&D group relative to the CON group. As depicted in Figure 3A–C, the therapeutic effect of the QYKL and Q&D groups was substantially more significant than that of the CON group based on the incidence of ALI/ARDS, pleural effusion, and the mortality rate. Regarding secondary efficacy indicators, such as duration of abdominal pain, duration of abdominal distension, and incidence of aberrant bowel sounds, the therapeutic effect of the QYKL and Q&D groups was also superior to that of the CON group (Figure 3D–F). In addition, QYKL and Q&D therapies decreased ICU occupancy and the use of mechanical ventilation (Figure 4A and B). Both the QYKL group and the Q&D group substantially reduced the duration of hospital stay and the length of stay in the ICU (Figure 4C and D). There were no significant differences between the two groups regarding hematological assays, including Amy, Lps, WBC#, and Neut#. For specifics regarding the data for each cohort, please refer to Supplementary Tables S8–S13.

Identification of the ingredients absorbed into the serum of QYKL

UHPLC-QE-MS was used to isolate and identify the chemical constituents of blank serum, rat serum after the oral administration of QYKL, and QYKL extract. Specifically, the chemical components of QYKL and rat serum were identified using retention time, precise relative molecular mass, secondary mass spectrometry lysate fragments, and database comparison. See Supplementary Figure S2 for the total ion chromatogram. A comprehensive scan for positive and negative ions detected 126 chemical components from QYKL. Please refer to Supplementary Table S14 for further details. As far as we know, 126 is the highest number of QYKL components presently detected using mass spectrometry. Analyses using PCA and OPLS-DA revealed that QYKL significantly altered the compounds in rat serum. We identified 23 prototype constituents of QYKL in rat serum by setting thresholds for VIP and P values and matching them with 126 specified chemical components of QYKL, as shown in Table 1.

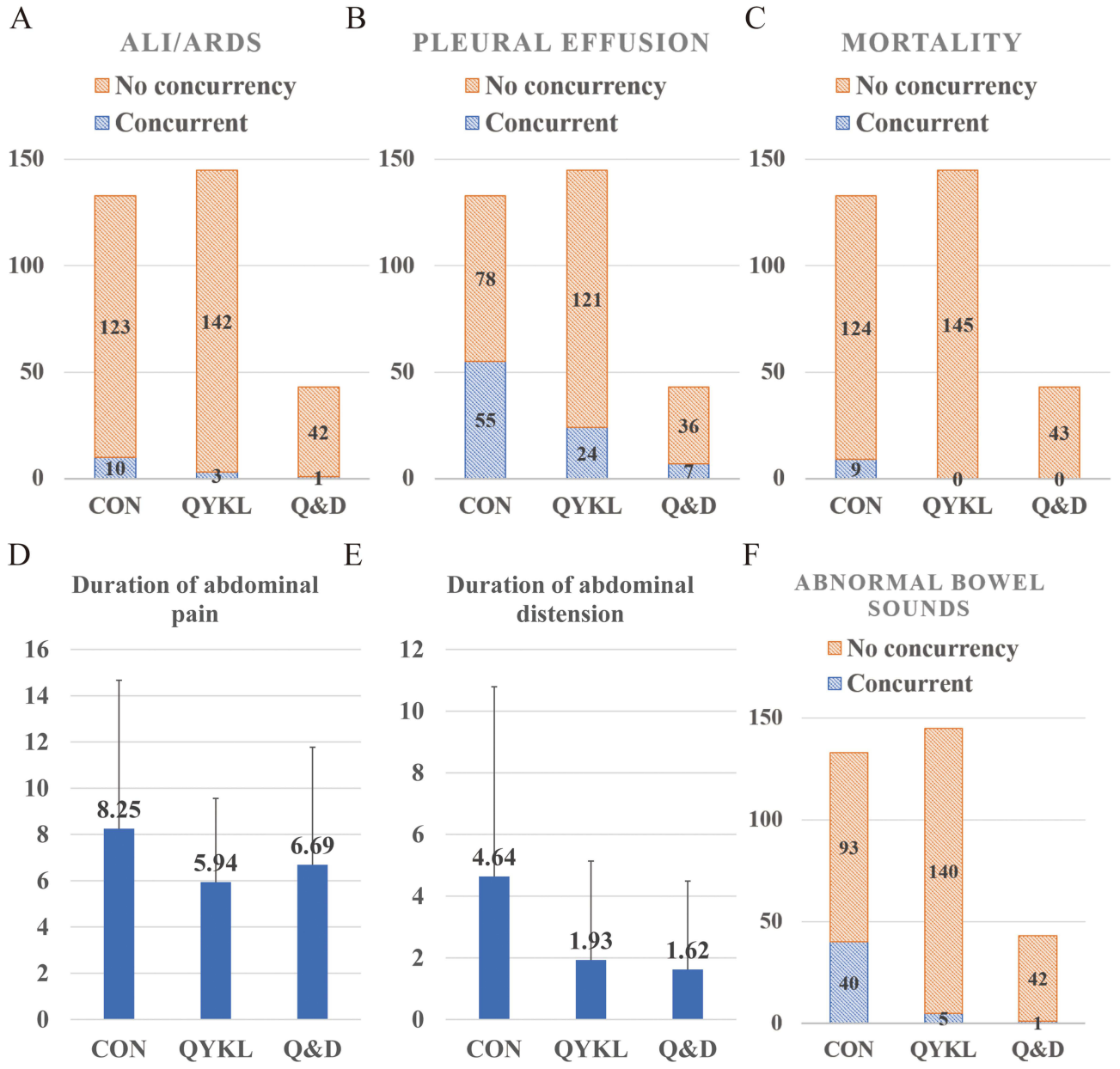

Figure 3 Comparison of primary and secondary clinical indicators. (**A**) ALI/ARDS. (**B**) Pleural effusion. (**C**) Mortality. (**D**) Duration of abdominal pain. (**E**) Duration of abdominal distension. (**F**) Abnormal bowel sounds.

Network Pharmacology

The bioavailability of each prototype component was queried using the SwissADME database. Flavone base + 3O, O-HexA (NorO > 10, NHorOH > 5) was precluded from the follow-up mechanism investigation based on the Lipinski rules (Table 1). Although quercetin-3-O-galactoside, scutellarin, and kaempferol-3-O-glucoside do not meet the Lipinski rules, their biological activities have been reported in some publications, so they are being studied further. Query the target of 22 prototype constituents from SwissTargetPrediction, TCMSP, and HERB databases. Finally, a total of 551 candidate targets were discovered and screened.

We employed the WGCNA algorithm to create co-expression gene networks related to SAP. Initially, a hierarchical clustering diagram is constructed for the samples, taking into account their correlation. The height was set to 50, and an outlier sample was removed for analysis (Figure 5A). A higher R^2 value indicates a more vital conformity of the model to

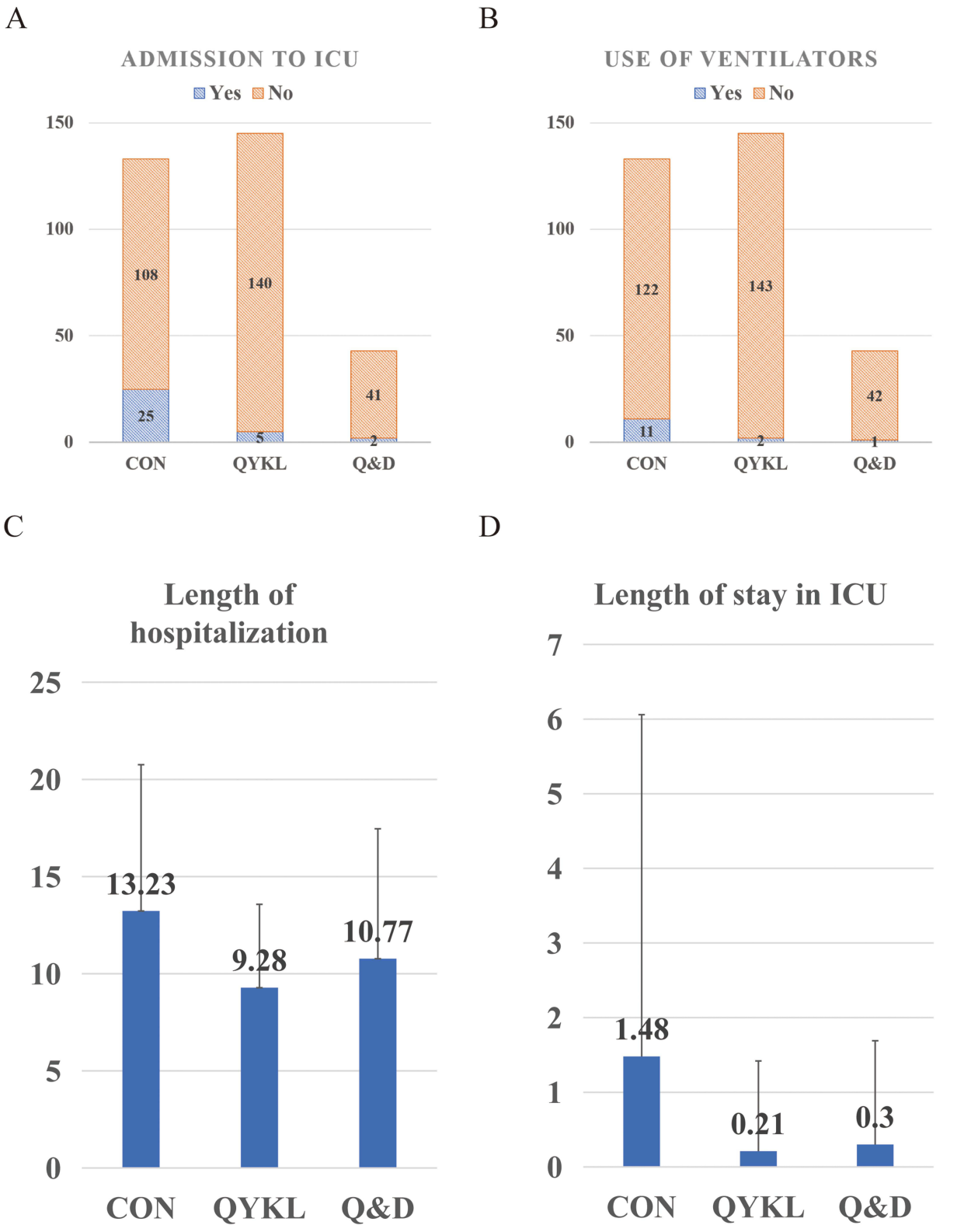

Figure 4 ICU Admissions and Use of Mechanical Ventilation. (**A**) Admission to ICU. (**B**) Use of ventilators. (**C**) Length of hospitalization. (**D**) Length of stay in ICU.

the scale-free distribution. Usually, R^2 should exceed 0.8, and in this study, a criterion of 0.85 was employed. The appropriate soft threshold is 11, as shown in Figure 5B when the fitting index R^2 is 0.85. Figure 5C illustrates that the dynamic shear tree approach was used to segment the modules and generate the network diagram. The consensus is

Table 1 23 Prototype Components in the Serum of Orally Administered QYKL Rats

Name	Class	HerbSet	Lipinski
Baicalin methyl ester	Flavonoids	a	Yes; 1 violation: NorO>10
Quercetin-3-O-galactoside	Flavonoids	b; c; d	No; 2 violations: NorO>10, NHorOH>5
Chrysophanol 8-O-beta-D-glucoside	Quinones	e	Yes; 0 violation
Rhein	Quinones	e	Yes; 0 violation
Scutellarin	Flavonoids	a	No; 2 violations: NorO>10, NHorOH>5
Laxapur	Quinones	e	Yes; 0 violation
Wogonoside	Flavonoids	a; d	Yes; 1 violation: NorO>10
Flavone base + 3O, O-HexA	Flavonoids	a; d; f	No; 2 violations: NorO>10, NHorOH>5
Daidzein-8-C-glucoside	Flavonoids	d	Yes; 1 violation: NHorOH>5
Kaempferol-3-O-glucoside	Flavonoids	f	No; 2 violations: NorO>10, NHorOH>5
Tetrahydrocoptisine	Alkaloids	c	Yes; 0 violation
Benzoic acid	Phenols	f	Yes; 0 violation
Gallic acid	Phenols	e; f	Yes; 0 violation
Chrysoeriol	Flavonoids	a	Yes; 0 violation
Corydaline	Alkaloids	c	Yes; 0 violation
Diethyl-phthalate	Benzoic acids and derivatives	d	Yes; 0 violation
Trans-4-Coumaric acid	Phenylpropanoids	a	Yes; 0 violation
Rhaponticin	Phenols	e	Yes; 1 violation: NHorOH>5
Methyl gallate	Phenols	f	Yes; 0 violation
Mifepristone	Terpenoids	a	Yes; 1 violation: MLOGP>4.15
(+)-Costunolide	Sesquiterpenoids	g	Yes; 0 violation
Afzelin	Flavonoids	a	Yes; 1 violation: NHorOH>5
Isoliquiritigenin	Flavonoids	d	Yes; 0 violation

Notes: a: Scutellaria baicalensis. b: Fructus Gardeniae. c: Rhizoma corydalis. d: Radix bupleuri. e: Rheum officinale. f: Radix paeoniae alba. g: Costustoot.

divided into 9 modules. The gray module denotes the set of genes not amenable to clustering. The association between each module and SAP is depicted in Figure 5D. The modules with the maximum correlation coefficient and P value less than 0.05 were regarded as SAP-specific, namely green modules (cor = 0.79, P < 0.01). Calculate the green module's GS and MM values and draw a scatter diagram (Figure 5E); the result shows that the green module strongly correlates with GS and MM (cor = 0.64, P < 0.01). The results of WGCNA suggest that the green module serves a crucial role in the SAP, and there is a strong correlation between 129 co-expressed genes and SAP-related ALI.

In addition, we identified 1478 APALI-related DEGs from the GSE151572 dataset (Figure 6A). After combining the green module genes obtained by green module-related genes and DEGs, 1558 final APALI-related genes were obtained (Figure 6B). We received 57 shared targets for the prototype constituents with APALI. Import the shared target into the DAVID database. With a P value less than 0.05 as the screening condition, 570 items were screened. There are 489 biological process (BP) items, 7 cellular component (CC) items, and 47 entries on molecular function (MF). Draw bar graphs of the top 10 BP, 7 CC, and 10 MF entries, as shown in Figure 6C. There are 27 pathways in the enrichment analysis of the KEGG pathway, and the top 10 pathways are displayed in bar charts in Figure 6D.

The interaction information between 57 nodes was obtained from the STRING database. A component-target network (79 nodes and 132 edges) was created using Cytoscape 3.8.2 software (Figure 6E). Then, the top 10 core targets, including estrogen receptor (ESR1), matrix metalloproteinase-9 (MMP9), vascular endothelial growth factor receptor 2 (KDR), xanthine dehydrogenase (XDH), equilibrative nucleoside transporter 1 (SLC29A1), PIM1, tyrosine-protein phosphatase non-receptor type 1 (PTPN1), multistage anoxic and oxic biofilm (MAOB), enzyme quinone reductase 2 (NQO2), and dipeptidyl peptidase 4 (DPP4) and top 10 compound, including corydaline, rhein, tetrahydrocoptisine, chrysophanol 8-O-beta-D-glucoside (Pulmatin), trans-4-coumaric acid, chrysoeriol, isoliquiritigenin, kaempferol-3-O-glucoside, laxapur, and wogonoside were identified.

The top 10 prototype components and the top 10 targets underwent molecular docking. Most ligand-receptor pair binding energies are below 7.0 kcal/mol (Supplementary Table S15). According to conventional wisdom, a small

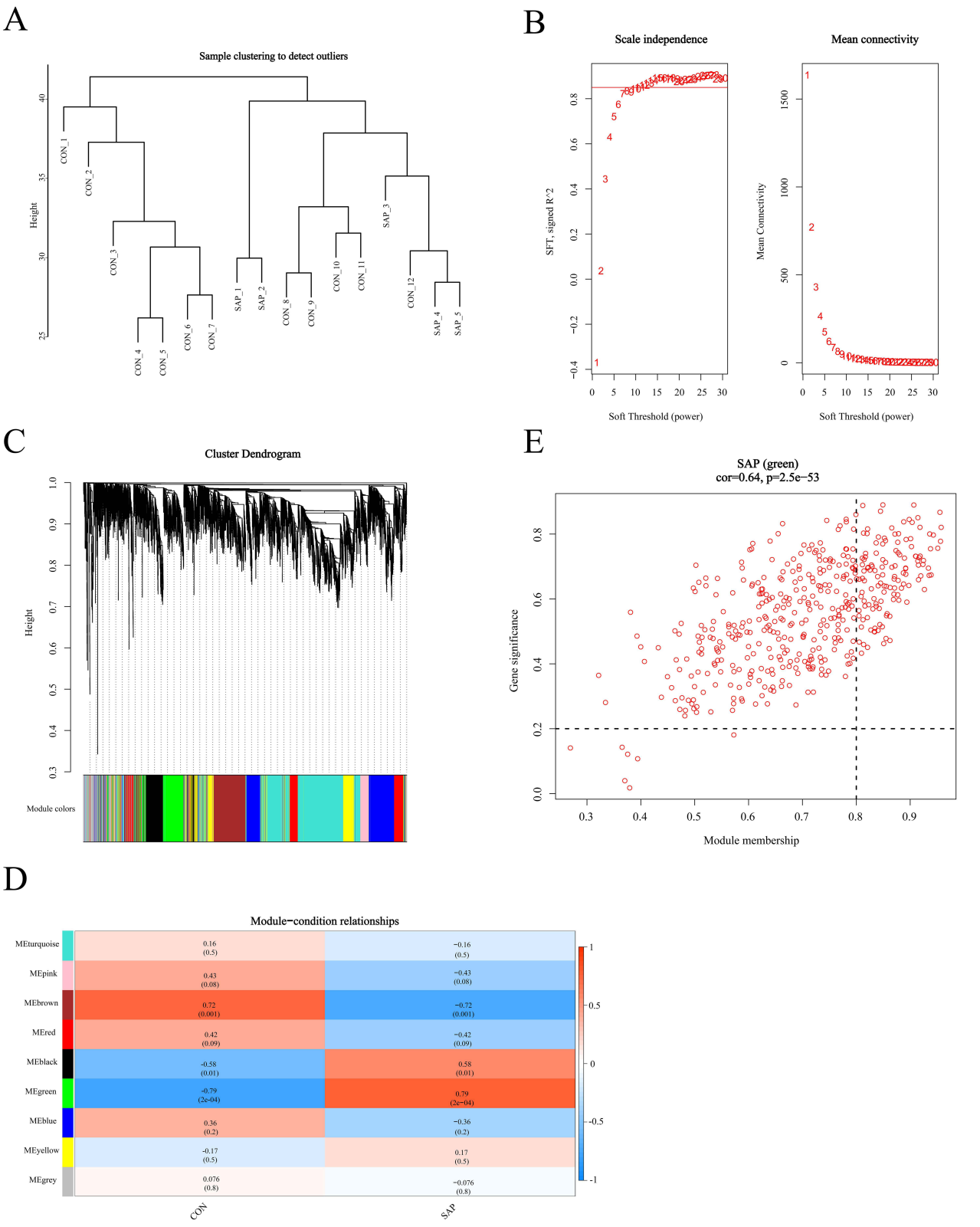

Figure 5 Construction of WGCNA network. (**A**) Cluster analysis of all samples. (**B**) The appropriate soft threshold is 11 when the fitting index R^2 is 0.85. (**C**) Gene hierarchy tree-clustering graph. (**D**) The module correlation heat map. (**E**) The green module's GS and MM values.

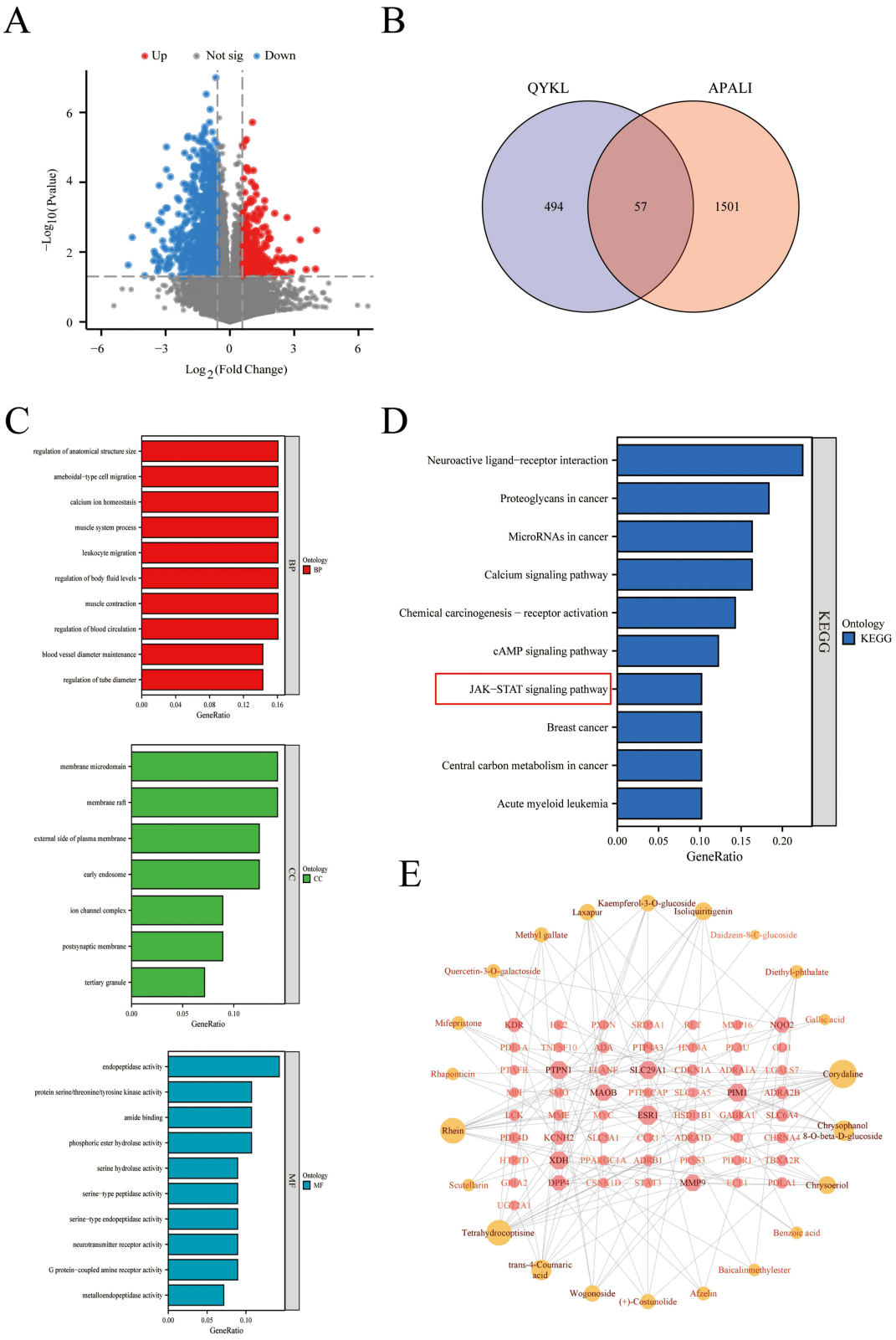

Figure 6 Identification and functional enrichment of APALI-related differentially expressed genes (DEGs). (**A**) The volcano plot of APALI-related DEGs. (**B**) The Venn diagram of DEGs and green module genes. The top 10 biological process, molecular function, and cellular component (**C**) items of shared targets. (**D**) The top 10 pathways of shared targets. (**E**) Prototype component and target network.

molecule has a stable binding activity with the target if its binding energy is less than 5 kcal/mol and a strong binding activity if it is less than 7.0 kcal/mol.[18]

QYKL combined with DEX alleviates pancreas injury and inflammation in SAP rats

Different dosages of QYKL significantly reduced the pancreas damage induced by SAP, with the medium dose of QYKL-M having the highest impact, and the effect was further strengthened after combination treatment with DEX. The H&E staining of the SAP group's pancreatic tissue revealed obvious bleeding, edema, necrosis, and inflammation, which were typical pathological features of SAP, whereas the application of QYKL significantly improved these pathological changes, with the QYKL-M+DEX group having the lightest pancreatic pathological injury degree (Figure 7A). In the serum amylase detection, different doses of QYKL reduced the amylase level, and the lowering impact was more substantial when paired with DEX (Figure 7B). The levels of inflammatory cytokines IL-1β and TNF-α in the SAP group were significantly higher than in the SO group, and they decreased in a dose-dependent manner after QYKL administration, with the inflammatory level being lowest after adding DEX to the medium dose of QYKL (Figure 7C and D). These findings suggest that combining QYKL and DEX can improve the treatment effect of QYKL alone on pancreatic damage in SAP rats.

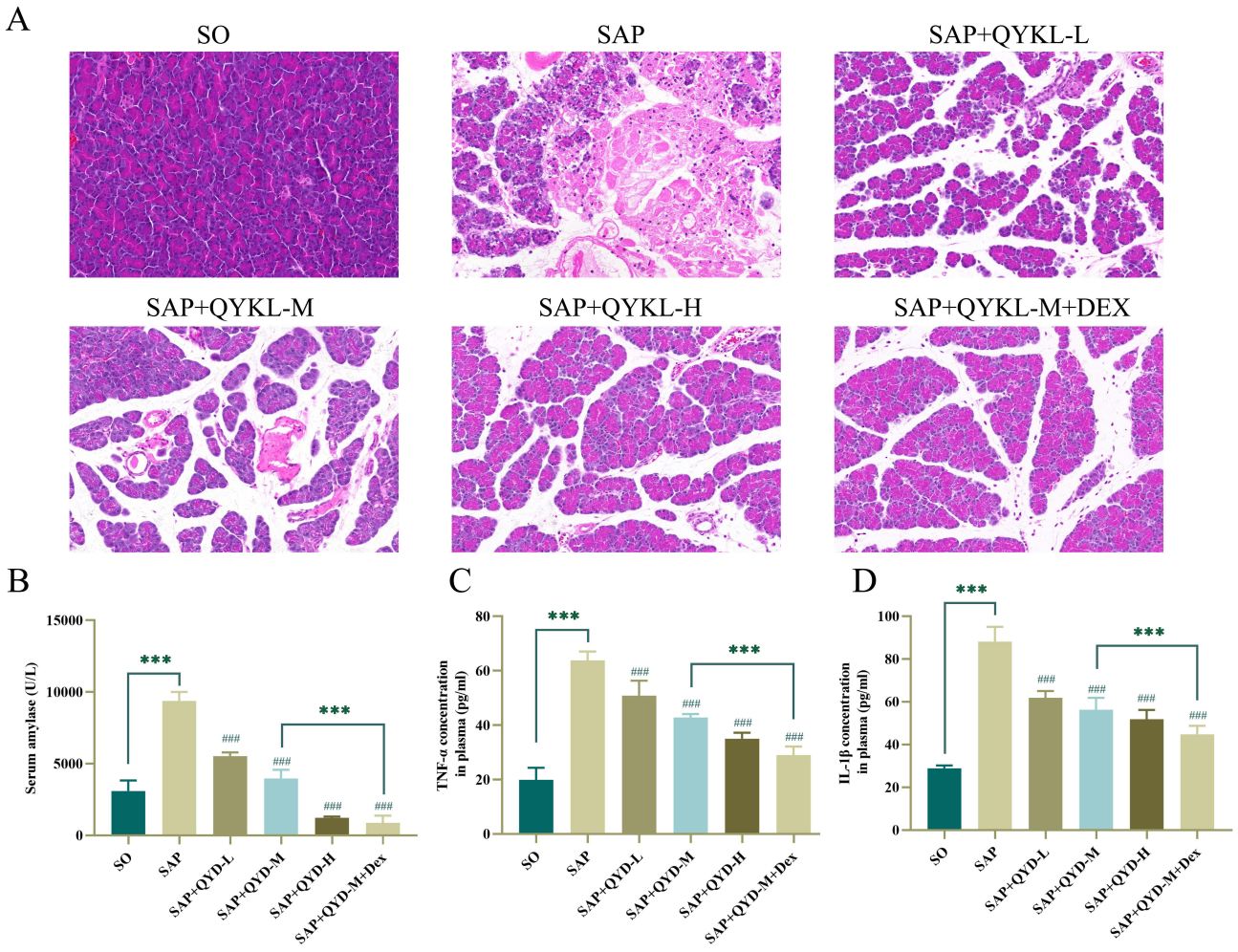

Figure 7 QYKL and DEX alleviated pancreatic injury and inflammation in the SAP rats. (**A**) H&E staining to evaluate the pathological damage of pancreatic tissue in rats (Scale bar = 100 μm). (**B**) Determination of serum amylase levels. Determination of serum TNF-α (**C**) and IL-1β (**D**) levels. Data were representative images of each group of rats in at least three independent experiments or expressed as mean±SD. *** indicates a P value less than 0.001. ### indicates a P value less than 0.001 compared to the SAP group.

QYKL Combined with DEX Alleviates Lung Injury and Respiratory Dysfunction in SAP Rats

The H&E staining of lung tissue revealed that, compared to the SO group, the SAP group displayed apparent pulmonary edema, leukocyte infiltration, and alveolar bleeding, all relieved by QYKL or QYKL-M+DEX therapy (Figure 8A). According to the arterial blood gas measurement results, the PaO_2 of the SAP group was lower than that of the SO group and increased following QYKL administration. The PaO_2 of the medium dosage QYKL group was the highest, equivalent to the combination therapy with DEX (Figure 8B). Regarding $PaCO_2$, which also represents a respiratory function, the SAP group's $PaCO_2$ was considerably more significant than the SO group's, showing CO_2 retention, and it reduced dose-dependently following QYKL administration. The $PaCO_2$ of the high-dosage QYKL group was the lowest, equivalent to the combination therapy with DEX (Figure 8C). Finally, we employed the lung W/D ratio to assess the degree of pulmonary edema, and the findings revealed that the SAP group's W/D ratio was considerably more significant than the SO group's, and it reduced dose-dependently after QYKL administration. The W/D ratio was lowest in the high-dosage QYKL group and the combination therapy with DEX (Figure 8D). These findings suggest that combining QYKL and DEX can improve the preventive effect of QYKL alone on lung damage in SAP rats.

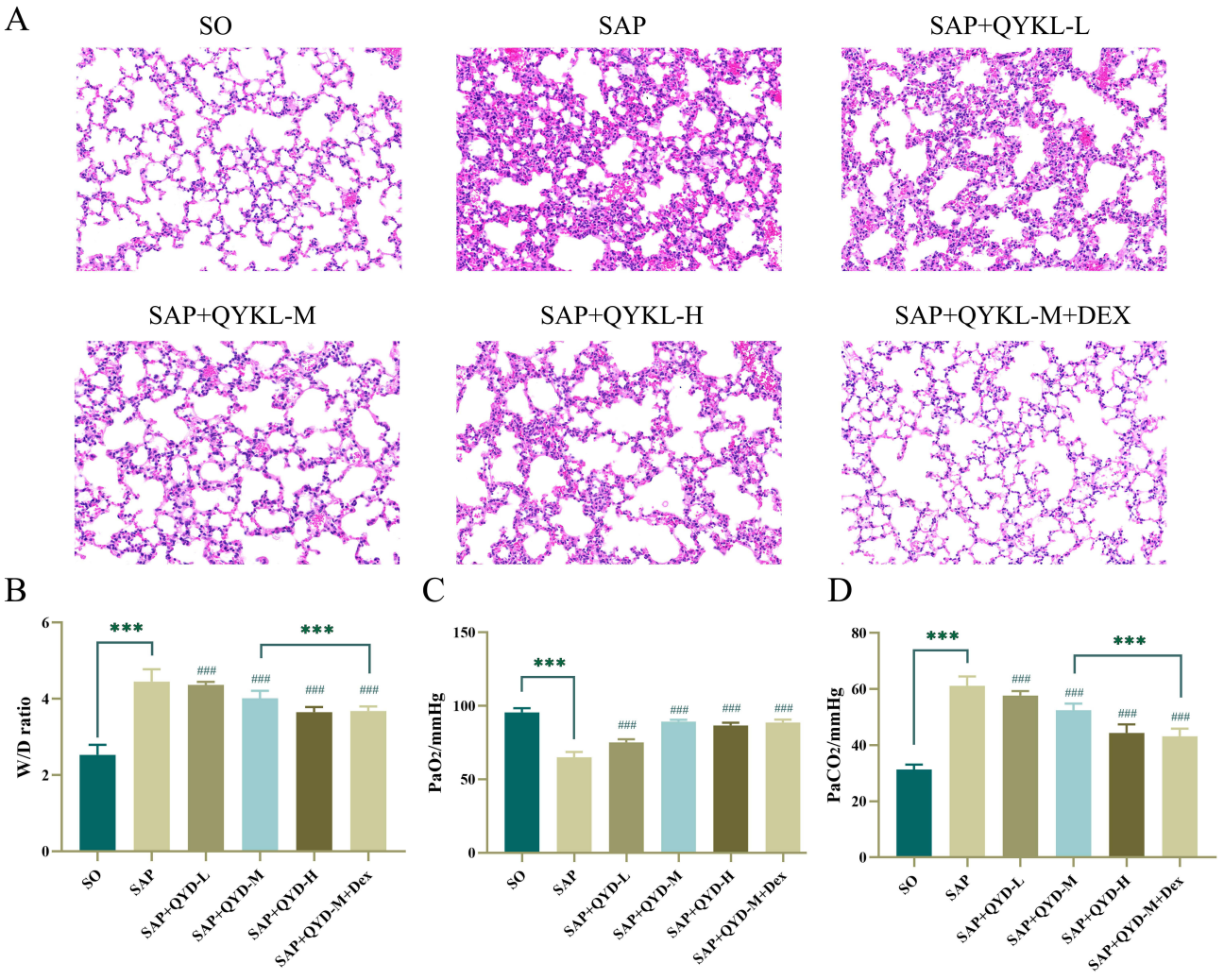

Figure 8 QYKL and DEX alleviated pulmonary tissue injury and respiratory function in the SAP rats. (**A**) H&E staining to evaluate the pathological damage of lung tissue in rats (Scale bar = 100 μm). (**B**) Comparison of W/D ratio of lung tissue. (**C** and **D**) Blood gas analysis. Data were representative images of each group of rats in at least three independent experiments or expressed as mean±SD. ***Indicates a P value less than 0.001. ###Indicates a P value less than 0.001 compared to the SAP group.

Effect of QYKL Combined with DEX on IL-6/STAT3 Signaling Pathway

The SAP group had substantially elevated IL-6 mRNA and phosphorylated STAT3 protein levels in lung tissue compared to the SO group (Figure 9A and B). After administration of QYKL, the level of IL-6 mRNA and phosphorylated STAT3 protein. The QYKL and DEX combination has the most significant effect (Figure 9C).

Discussion

MR Analysis

We proposed the pancreas-intestine-inflammation/endotoxin-lung pathway (P-I-I/E–L pathway) in 2020.[19] Inflammatory cytokines play a central role in the pathological process of AP and mediate the ARDS caused by systemic inflammation. Our MR analysis does not support a causal link between AP/AAP and ARDS/pleural effusion/pulmonary edema. We speculate that the contradiction between the negative results of MR analysis and the conclusion of the previous study that SAP is the cause of ALI has multiple reasons. On the one hand, the early manifestation of AP is mainly local inflammation of the pancreas and rarely induces MODS, represented by respiratory failure. AP and SAP are separate phases of the illness, with significantly different pathophysiology and prognosis, and it is hard to evaluate whether there is a direct causative association between SAP and ALI/ARDS owing to a lack of aggregated GWAS results for SAP. Previous research suggests that AP primarily causes ARDS by mediating cytokine storms. Consequently, we evaluated the influence of AP on cytokines. We found that AP/AAP substantially increased the levels of IL-1 and IL-4 in the circulation, suggesting that AP may activate the cytokine storm, thereby inducing ALI/ARDS. Nevertheless, our MR analysis is subject to a few limitations. The GWAS summary data included in this study were only derived from European populations. Therefore, it is essential to conduct further verification to ascertain the applicability of causal estimates to other populations. Furthermore, despite the relaxation of the screening criterion for SNPs, including a limited number of IVs may compromise internal validity and raise concerns about the degree to which IVs may account for a small percentage of overall explanations for exposure. We used MR analysis to assess the absence of weak IV bias by

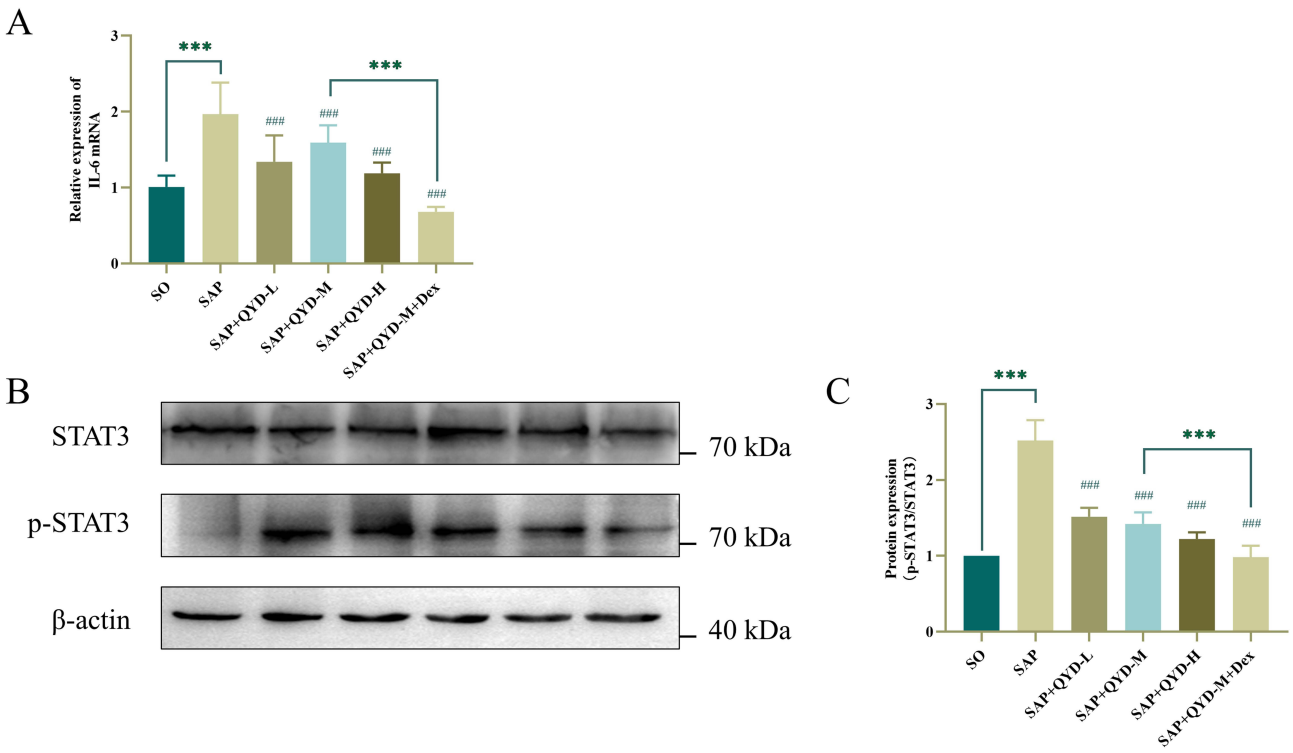

Figure 9 Inhibitory effect of QYKL and DEX on IL-6/STAT3 signaling pathway in SAP rats. IL-6 mRNA (**A**) and STAT3/p-STAT3 protein expression (**B** and **C**) levels in rat lung tissues were measured by qRT-PCR and WB. Data were representative images of each group of rats in at least three independent experiments or expressed as mean ±SD. ***Indicates a P value less than 0.001. ###Indicates a P value less than 0.001 compared to the SAP group.

calculating the F statistic. Additionally, we employed several approaches to ascertain the absence of pleiotropy and heterogeneity among the IVs. Nevertheless, despite these efforts, it is impossible to entirely eradicate mistakes resulting from selection bias, consistency problems, and pleiotropy. In summary, more data and statistical methodologies are required in further investigations to assess the dependability of the causal estimations derived from this work.

Retrospective Study

The QYKL group in this study showed decreases in ALI/ARDS, the incidence of pleural effusion, and mortality compared with the patients who had conventional treatment, as well as had a more significant decrease in the incidence of pleural effusion after the combination of DEX. DEX sodium phosphate is a commonly used, long-acting glucocorticoid (GC).[20–23] The European Society of Intensive Care Medicine and the Corticosteroid Guideline Task Force of the Society of Critical Care Medicine (SCCM) issued guidelines for the use of GC treatment in ARDS patients in 2017.[24] We found that the early application of QYKL or QYKL combined with DEX significantly reduced the ICU admission rate and the use of mechanical ventilation, with only 5 patients (3. 4%) in the QYKL group and 2 patients (4. 7%) in the Q&D group needing ICU admission, which are significantly lower numbers than the 25 patients (18. 8%) in the CON group. This indicates that the QYKL and Q&D groups were more likely to have a significantly improved prognosis. In the observation of patients with SAP who eventually died due to infection necrosis, respiratory failure, and MODS, both the QYKL and Q&D groups demonstrated the clinical value of the early application of pancreatic granules or pancreatic granules combined with DEX for the treatment of AP because of their meager mortality rate of 0. 0% ($P < 0. 05$) compared to the CON group, which had a mortality rate of 6. 8%. DEX also significantly reduced hospitalization costs by reducing the length of hospitalization and the duration of ICU admission. In a word, the results all indicated that the synergistic impact of QYKL and DEX might provide unexpected advantages in treating SAP-related ALI patients.

Mass Spectrometry and Network Pharmacology

The chemical components of QYKL and the prototype constituents absorbed into serum were identified by liquid mass spectrometry. 126 chemical components of QYKL have been identified. As the main component of Qingyi Decoction, emodin can significantly improve ALI caused by SAP. Our team previously demonstrated the mechanism of action of EMO to improve SAP-related ARDS by inhibiting macrophage pyroptosis[25] and promoting neutrophil apoptosis.[26] Additionally, we identified 23 prototype constituents of QYKL that were absorbed into the serum. Rhein, one of the anthraquinone compounds in the prototype constituents, has also been shown to have anti-AP properties. Previous research suggested that rhein and honokiol could regulate metabolic disorders and mitigate AP's pancreatic damage.[27] Experiments using rhein alone to treat AP in rats and AR42J cell lines showed that it could reduce inflammation and damage to acinar cells by inhibiting the JAK2/STAT3 signaling cascade.[28] The flavonoid quercetin-3-O-galactoside, also known as hyperin, has shown promise as a therapeutic medication for ALI due to its ability to reduce LPS-induced pulmonary inflammation and damage.[29] The prototype constituents also include scutellarin, a flavonoid. Scutellarin has been shown to reduce SAP-induced harm to several organs significantly.[30] Scutellarin is involved in the recovery from LPS-induced ALI by decreasing the severity of mitochondrial malfunction, oxidative stress, and parenchymal cell excessive apoptosis.[29] In other words, anthraquinones and flavonoids are the main components of QYKL against AP and related ALI. In addition, APALI-related genes were identified through DEG analysis and WGCNA using publicly available data sets. Following the intersection with the prototype constituent target, 57 genes were found to be shared. JAK-STAT signaling pathway and cAMP signaling pathway were identified as the main pathways of QYKL against APALI. The primary targets of QYKL were ESR1, MMP9, KDR, XDH, SLC29A1, PIM1, PTPN1, MAOB, NQO2, and DPP4. Molecular docking demonstrated the strong binding ability of the prototype components to key targets.

Animal Experiment

In the animal experiment, we assessed the pancreatic and pulmonary pathologies and arterial blood gas, amylase, and inflammatory cytokines (IL-1β, TNF-α) levels. Although the levels of inflammatory cytokines (IL-1β, TNF-α) in the high-dose QYKL group were the lowest, considering the conventional dose and toxic side effects, we still regarded the medium-dose QYKL group as the standard dose. We found that after combined treatment with DEX, the inflammatory

cytokines levels decreased further. Consistent with our clinical findings, QYKL paired with DEX therapy improved pancreatic and pulmonary damage markers in the animal model, such as tissue pathology, blood gas, amylase, and lung wet/dry weight ratio, among others, and did so better than the QYKL group. In previous studies, Chen et al shown that QYKL and DEX could successfully reduce secreted phospholipase A_2 ($sPLA_2$), AMY, TNF-α, and diamine oxidase overexpression and restore intestinal function damage.[31] Subsequent target mining uncovered the crucial function of the STAT3 signaling pathway. STAT3 is one of seven members of the signal transducer and activator of the transcription (STAT) family. Injuries to the pancreas, intestine, liver, and lungs caused by AP have been linked to abnormal activation of STAT3.[32–34] Regulating STAT3 activity has been proposed as a therapy method for AP by many studies. IL-6 is a crucial inducer that induces STAT3 activation. We measured the IL-6 mRNA level and phosphorylation STAT3 protein in lung tissue. The results suggested that QYKL alone or QYKL combined with DEX could substantially inhibit SAP-induced activation of the IL-6/STAT3 signaling pathway.

Conclusion

Our MR analysis bolsters the conclusion that cytokine storm is a key mechanism underlying SAP-mediated ALI/ARDS. Specifically, inflammatory markers such as IL-6 and IL-1β are important pathogenesis factors. After collecting and analyzing previous case data from 321 patients with acute pancreatitis, it was observed that the leading efficacy indicators (mortality, incidence of ARDS/ALI) were significantly reduced after the early application of Qingyi granules. In addition, some of the symptoms, laboratory indices, and economic benefits were also considerably better with the use of dexamethasone combined with Qingyi granules. We identified that the prototype constituents of QYKL absorbed into the blood are mainly flavonoids (quercetin-3-O-galactoside, chrysophanol 8-O-beta-D-glucoside, and scutellarin) and anthraquinones (rhein). In vivo experiments prove the superior efficacy of the combination of QYKL and DEX compared to QYKL alone in treating rats with SAP, which may play anti–inflammatory effects by regulating IL-6/STAT3 signal pathway.

The risks and benefits should be considered when evaluating the different treatment methods. Although our study have shown that GC has a general effect on AP and its complications, many reports also show that long-term low-to-medium doses of GC downregulate the life-threatening inflammatory response. At the same time, it also provides a favorable environment for the growth of bacteria, and the immunosuppression induced by GCs is one of the leading causes of secondary infections. Although AP patients can benefit from GC administration, many adverse events caused by GC, such as osteoporosis, wound healing difficulties, and gastrointestinal bleeding, are still worthy of our attention.

Data Sharing Statement

The manuscript and Supplementary Materials include all of the study's data.

Ethics Approval and Consent to Participate

The studies involving human participants were reviewed and approved by the Ethics Committee of the First Affiliated Hospital of Dalian Medical University and were performed according to the Declaration of Helsinki's ethical principles. The in vivo experiments were reviewed and approved by the Experimental Animal Ethics Committee of Dalian Medical University.

Acknowledgment

Peng Ge, Yalan Luo, and Jinquan Zhang are co-first authors for this study. We want to acknowledge the participants and investigators of the FinnGen consortium and MRC Integrative Epidemiology Unit.

Funding

This study was supported by the National Key R&D Program of China (No. 2019YFE0119300) and the National Natural Science Foundation of China (NO. 82274311, 82074158, and 82104594).

Disclosure

We have no financial relationships to disclose.

References

1. Petrov MS, Yadav D. Global epidemiology and holistic prevention of pancreatitis. *Nat Rev Gastroenterol Hepatol*. 2019;16(3):175–184. doi:10.1038/s41575-018-0087-5
2. Fagenholz PJ, Fernández-del Castillo C, Harris NS, et al. Direct medical costs of acute pancreatitis hospitalizations in the United States. *Pancreas*. 2007;35(4):302–307. doi:10.1097/MPA.0b013e3180cac24b
3. Renner IG, Savage WT, Pantoja JL, Renner VJ. Death due to acute pancreatitis. A retrospective analysis of 405 autopsy cases. *Dig Dis Sci*. 1985;30:1005–1018. doi:10.1007/BF01308298
4. Yu P, Zeng QQ, Wang HC, et al. Efficacy of Qingyi decoction in the treatment of severe acutepancreatitis: systematic review and meta-analysis. *J Pra Med*. 2008;2008:544–547.
5. Li L, Li YQ, Sun ZW, et al. Qingyi decoction protects against myocardial injuries induced by severe acute pancreatitis. *World J Gastroenterol*. 2020;26(12):1317–1328. doi:10.3748/wjg.v26.i12.1317
6. Su S, Liang T, Zhou X, et al. Qingyi decoction attenuates severe acute pancreatitis in rats via inhibition of inflammation and protection of the intestinal barrier. *J Int Med Res*. 2019;47(5):2215–2227. doi:10.1177/0300060518809289
7. Wang G, Shang D, Zhang G, et al. Effects of QingYi decoction on inflammatory markers in patients with acute pancreatitis: a meta-analysis. *Phytomedicine*. 2021;95:153738. doi:10.1016/j.phymed.2021.153738
8. Wei TF, Zhao L, Huang P, et al. Qing-Yi decoction in the treatment of acute pancreatitis: an integrated approach based on chemical profile Network Pharmacology, Molecular Docking and Experimental Evaluation. *Front Pharmacol*. 2021;12:590994.
9. Ge P, Luo Y, Yang Q, et al. Ferroptosis in rat lung tissue during severe acute pancreatitis-associated acute lung injury: protection of qingyi decoction. *Oxid Med Cell Longev*. 2023;2023:5827613. doi:10.1155/2023/5827613
10. Zhang H. Pros and cons of Mendelian randomization. *Fertil Steril*. 2023;119(6):913–916. doi:10.1016/j.fertnstert.2023.03.029
11. Ahola-Olli AV, Würtz P, Havulinna AS, et al. Genome-wide association study identifies 27 loci influencing concentrations of circulating cytokines and growth factors. *Am J Hum Genet*. 2017;100(1):40–50. doi:10.1016/j.ajhg.2016.11.007
12. Daina A, Michielin O, Zoete V. SwissADME: a free web tool to evaluate pharmacokinetics, drug-likeness and medicinal chemistry friendliness of small molecules. *Sci Rep*. 2017;7:42717. doi:10.1038/srep42717
13. Ru J, Li P, Wang J, et al. TCMSP: a database of systems pharmacology for drug discovery from herbal medicines. *J Cheminform*. 2014;6:13. doi:10.1186/1758-2946-6-13
14. Daina A, Michielin O, Zoete V. SwissTargetPrediction: updated data and new features for efficient prediction of protein targets of small molecules. *Nucleic Acids Res*. 2019;47:W357–W364. doi:10.1093/nar/gkz382
15. Sun Z, Li L, Qu J, Li H, Chen H. Proteomic analysis of therapeutic effects of Qingyi pellet on rodent severe acute pancreatitis-associated lung injury. *Biomed Pharmacother*. 2019;118:109300. doi:10.1016/j.biopha.2019.109300
16. Xu C, Luo Y, Ntim M, et al. Effect of emodin on long non-coding RNA-mRNA networks in rats with severe acute pancreatitis-induced acute lung injury. *J Cell Mol Med*. 2021;25(4):1851–1866. doi:10.1111/jcmm.15525
17. Definition Task Force ARDS, Ranieri VM, Rubenfeld GD, et al. Acute respiratory distress syndrome: the Berlin definition. *JAMA*. 2012;307(23):2526–2533. doi:10.1001/jama.2012.5669
18. Hsin KY, Ghosh S, Kitano H. Combining machine learning systems and multiple docking simulation packages to improve docking prediction reliability for network pharmacology. *PLoS One*. 2013;8(12):e83922. doi:10.1371/journal.pone.0083922
19. Ge P, Luo Y, Okoye CS, et al. Intestinal barrier damage, systemic inflammatory response syndrome, and acute lung injury: a troublesome trio for acute pancreatitis. *Biomed Pharmacother*. 2020;132:110770. doi:10.1016/j.biopha.2020.110770
20. Coutinho AE, Chapman KE. The anti-inflammatory and immunosuppressive effects of glucocorticoids, recent developments and mechanistic insights. *Mol Cell Endocrinol*. 2011;335(1):2–13. doi:10.1016/j.mce.2010.04.005
21. Salt AN, Plontke SK. Pharmacokinetic principles in the inner ear: influence of drug properties on intratympanic applications. *Hear Res*. 2018;368:28–40. doi:10.1016/j.heares.2018.03.002
22. Zen M, Canova M, Campana C, et al. The kaleidoscope of glucorticoid effects on immune system. *Autoimmun Rev*. 2011;10(6):305–310. doi:10.1016/j.autrev.2010.11.009
23. Zhang M, Moore GA, Jensen BP, et al. Determination of dexamethasone and dexamethasone s phosphate in human plasma and cochlear perilymph by liquid chromatography/tandem mass spectrometry. *J Chromatogr B Analyt Technol Biomed Life Sci*. 2011;879(1):17–24. doi:10.1016/j.jchromb.2010.11.003
24. Pastores SM, Annane D, Rochwerg B, et al. Guidelines for the diagnosis and management of critical illness-related corticosteroid insufficiency (CIRCI) in critically ill patients (Part II): society of Critical Care Medicine (SCCM) and European Society of Intensive Care Medicine (ESICM) 2017. *Intensive Care Med*. 2018;44(4):474–477. doi:10.1007/s00134-017-4951-5
25. Xu Q, Wang M, Guo H, et al. Emodin alleviates severe acute pancreatitis-associated acute lung injury by inhibiting the cold-inducible RNA-Binding Protein (CIRP)-mediated activation of the NLRP3/IL-1β/CXCL1 Signaling. *Front Pharmacol*. 2021:655372. doi:10.3389/fphar.2021.655372
26. Cui H, Li S, Xu C, et al. Emodin alleviates severe acute pancreatitis-associated acute lung injury by decreasing pre-B-cell colony-enhancing factor expression and promoting polymorphonuclear neutrophil apoptosis. *Mol Med Rep*. 2017;16(4):5121–5128. doi:10.3892/mmr.2017.7259
27. Huang W, Liu H, Li Y, Mai G. The effects of rhein and honokiol on metabolic profiles in a mouse model of acute pancreatitis. *Med Sci Monit*. 2020;26:e925727. doi:10.12659/MSM.925727
28. Yang X, Geng H, You L, et al. Rhein protects against severe acute pancreatitis in vitro and in vivo by regulating the JAK2/STAT3 pathway. *Front Pharmacol*. 2022;13:778221. doi:10.3389/fphar.2022.778221
29. Hu X, Li H, Fu L, et al. The protective effect of hyperin on LPS-induced acute lung injury in mice. *Microb Pathog*. 2019;127:116–120. doi:10.1016/j.micpath.2018.11.048

30. Hanqing C, Xiping Z, Jingmin O, Jun J, Dijiong W. Research on scutellarin parenteral solution's protective effects in rats with severe acute pancreatitis and multiple organ injuries. *Inflammation*. 2012;35:1005–1014. doi:10.1007/s10753-011-9404-7
31. Zhang JW, Zhang GX, Chen HL, et al. Therapeutic effect of Qingyi decoction in severe acute pancreatitis-induced intestinal barrier injury. *World J Gastroenterol*. 2015;21:3537–3546. doi:10.3748/wjg.v21.i12.3537
32. Li M, Zhang X, Wang B, et al. Effect of JAK2/STAT3 signaling pathway on liver injury associated with severe acute pancreatitis in rats. *Exp Ther Med*. 2018;16:2013–2021. doi:10.3892/etm.2018.6433
33. Qin MZ, Qin MB, Liang ZH, Tang GD. Effect of SOCS3 on lung injury in rats with severe acute pancreatitis through regulating JAK2/STAT3 signaling pathway. *Eur Rev Med Pharmacol Sci*. 2019;23:10123–10131. doi:10.26355/eurrev_201911_19582
34. Yang J, Han F, Wu G, et al. Dysregulated B7H4/JAK2/STAT3 pathway involves in hypertriglyceridemia acute pancreatitis and is attenuated by baicalin. *Dig Dis Sci*. 2023;68:478–486. doi:10.1007/s10620-022-07606-5